Hindawi Publishing Corporation
Active and Passive Electronic Components
Volume 2008, Article ID 537069, 8 pages
doi:10.1155/2008/537069

Research Article

Modeling and Measurements of Novel Monolithic Filters

Aly H. Aly,[1] Badawy El-Sharawy,[1] and Adalbert Beyer[2]

[1] *Department of Electrical Engineering, Arizona State University, Tempe, AZ 85287-7206, USA*
[2] *Department of Electrical Engineering and Communications, University of Duisburg-Essen, Campus Duisburg, 47057 Duisburg, Germany*

Correspondence should be addressed to Adalbert Beyer, adalbert.beyer@uni-duisburg-essen.de

Received 27 December 2007; Accepted 24 June 2008

Recommended by T. Kalkur

This paper presents novel multilayer tuneable high *Q*-filters based on hairpin resonators including ferroelectric materials. This configuration allows the miniaturization of these filters to a size that makes them suitable for chip and package integration and narrow-band applications. The main focus was miniaturizing filters with coupled loops using multilayer dielectric substrates. A further goal was to increase the quality factor of these distributed filters by embedding high dielectric materials in a multilayer high- and low-*k* (dielectric constant) substrate that is supported by LTCC technology. An improved W-shape bandpass filter was proposed with a wide stopband and approximately 5% bandwidth.

1. INTRODUCTION

At microwave frequencies, the parallel-coupled-resonator filters [1] and the hairpin resonator filters [2] are the most widely used filters because of their design, ease of fabrication, and low cost. However, these filters have some disadvantages such as: large size, high loss, especially when the number of coupled resonators is increased, low stopband rejection, and spurious response at the filter's harmonics.

Many filter topologies were explored using coupled-line theory in strip line and microstrip to improve the performance. A cross-coupled topology was proposed [3] to create controlled attenuation poles or transmission zeros by allowing different coupling paths with different phases for the input signal. These transmission zeros are created in the stopband either above, below, or between resonances to enhance filter rejection [4, 5]. A drawback of this technique is the high loss of the filter, especially when zeros are placed near the resonant frequency. Another drawback is the bandwidth asymmetry created from concentration of rejection on one stopband (above or below resonance) and relaxed on the other band. Different coupling schemes for resonator filters were introduced in [6].

Stepped impedance hairpin resonators were introduced in [7] to reduce the resonator size and enhance the performance. In [8], the hairpin resonator's length is further decreased by capacitive loading at the end of the resonator. The main disadvantage of capacitive loaded resonators is the high loss due to the increased resonator capacitance. This explains why all of the applications of this filter use high-temperature superconductors (HTSs) [9] which have a limited usage in wireless applications. Slow-wave open-loop resonators were presented in [10]. These allow for various elliptic and quasielliptic function responses to be realized at the expense of high insertion loss. This loss limits this filter to HTS applications. Another coupled-line filter using defected ground structure (DGS) was presented in [11] in which a defect in the ground plane below the coupled lines added more transmission zeros to the resonance characteristics of the filter. Utilizing this DGS may not be applicable in terms of filter integration and fabrication. Zigzag hairpin comb resonators have been proposed in [12], to further reduce the size, but the filter is suffering from a very high capacitance from winding the hairpin resonators. This winding increases the losses, which is why this filter was only utilized in HTS technology where conductor loss is of no concern.

Besides the improvement in the resonator structure, feed structures also play an important role in optimizing the performance the filters. Different feed topologies have been used such as: parallel-coupled-feed structure [1], tapped-line [13, 14], and the end-coupled feed structures. Most of the feed structures are capacitively coupled feeds or electric field

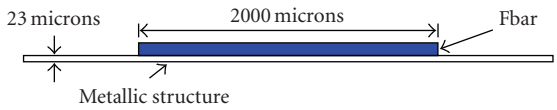

Figure 1: FBAR coupled to a microstrip line.

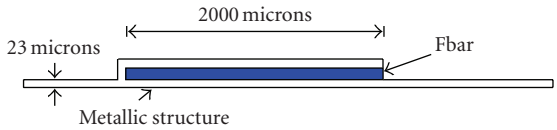

Figure 2: FBAR coupled to a microstrip hairpin with side coupling.

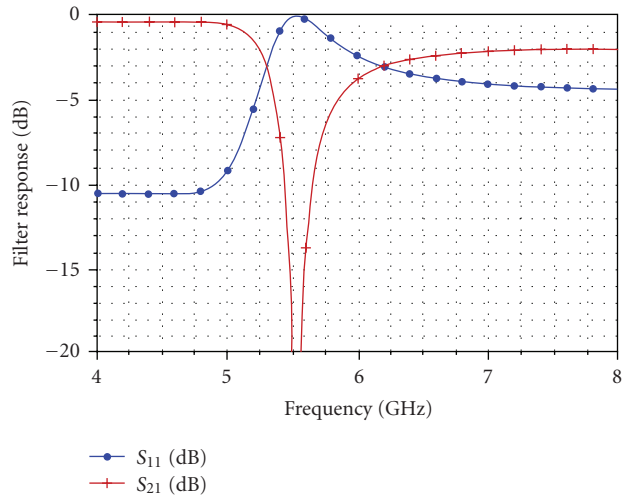

Figure 3: Frequency response of an FBAR coupled to a microstrip hairpin with side coupling.

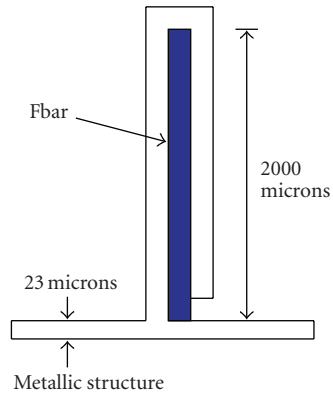

Figure 4: FBAR coupled to a hairpin with edge coupling.

coupling, which can increase the overall capacitance of the filter and reduce Q. Optimization of the feed location and length controls the strength of the coupling, which controls bandwidth and Q.

The progress and feasibility of filter integration are usually coupled to filter tuning. Electronic tuning is used to compensate for manufacturing and process variations. Ferroelectric materials have been suggested for both filter tuning and size reduction [15–17]. Most ferroelectric materials have relative dielectric constant greater than 200. There is a tradeoff between material Q and tunableness. Materials like $KTaO_3$ have high Q, greater than 10 000 but have poor tunableness of less that 1% per V/μm. The preferred choice has been $BaSrTiO_3$ which has a relative dielectric constant equal or greater than 5000 and tunableness of 20% per V/μm but has a poor Q of less than 100. The most common design is the lumped element filter with ferroelectric loaded capacitors [17]. This approach yields a low Q of less than 30 due to the low Q of the lumped elements.

This paper describes the properties of a multilayer dielectric mode filter coupled through hairpins to increase coupling and reduce size. Tight coupling is required to achieve low insertion loss. Medium k and high Q material, such as $KTaO_3$, is inserted between two layers of high k material such as $BaSrTiO_3$. The high k material pulls the fields inside the low k material to enhance both tunableness and Q. The present modes are EM dielectric modes in the ferroelectric material for the design of band-reject filter and oscillator applications.

Now, the paper is organized as follows. Section 2 describes some properties of the dielectric mode hairpin filters. In Section 3, the topic "multilayer filters" is treated. Section 4, an overview of the LTCC technology and the LTCC substrate configuration is shown. Section 5 presents the properties of hair-pin resonator filter. Section 6 presents the fabrication and measurements of different coupled-line filters, and the paper is concluded in Section 7.

2. DIELECTRIC MODE HAIRPIN FILTERS

Simple band-reject filters (BRFs) can be constructed using a dielectric resonator (DR) placed next to a microstrip line or by coupling ferroelectric bars made of $KTaO_3$ (with a relative dielectric constant of 240 and Q of about 10 000) to a 50 ohms microstrip line as shown in Figure 1. The present dimensions of the microstrip and ferroelectric bar are required for on-chip integration.

In order to increase the coupling and to enhance the filter characteristics, a hairpin is wrapped around the ferroelectric bar as shown in Figure 2.

The performance of the filter depicted in Figure 2 is calculated versus frequency using the HFSS software package from Ansoft, Pa, USA, and is shown in Figure 3.

A significant improvement in coupling and Q, as compared to the simple bar, is observed.

Next, the hairpin is coupled to the 50 ohms line at an edge of the hairpin as shown in Figure 4. Also the resonant frequency is reduced by a factor of 2 for the same bar dimension. When the field distribution is studied, it has been found that the loop of the hairpin produces a maximum magnetic field in the ferroelectric bar resulting in effectively a virtual ground at the loop. A maximum electric field occurs at the open end. Thus, the dimension of the resonant bar is reduced to $\lambda/4$ instead of $\lambda/2$ as compared to case of a conventional dielectric resonator. To verify the type of mode,

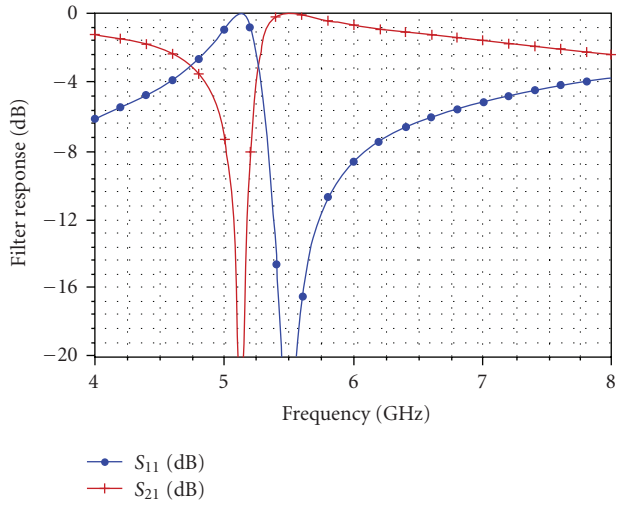

Figure 5: Frequency response of an FBAR coupled to a hairpin with edge coupling.

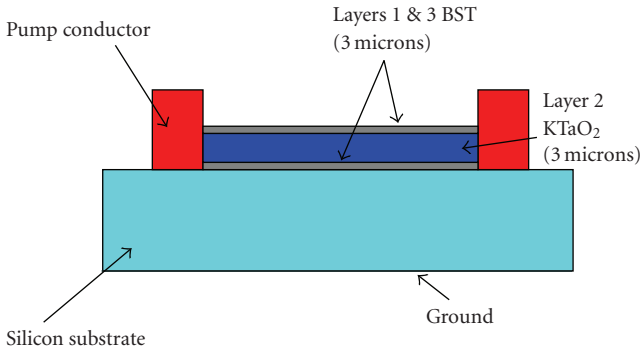

Figure 6: Geometry of a multilayer BRF.

the hairpin is coupled to the 50 ohms line at an edge of the hairpin as shown in Figure 4. The resonant frequency did not change significantly, as shown in Figure 5.

3. MULTILAYER FILTERS

The material, which is used in the above-described devices as ferroelectric bars, is made of $KTaO_3$ (with a relative dielectric constant of 240 and Q of about 10 000), and it has a very poor tuning, but fairly high Q. In order to increase the tunableness, another material, namely, a $BaSrTiO_3$ layer can be used in conjunction with $KTaO_3$ as shown in Figure 6. Thus, multilayer filter structures may be obtained.

In all of following simulations, a silicon dioxide substrate was used with an effective dielectric constant of 4 and a thickness of 15 μm which gives a 50-ohms microstrip line of 23 μm width. The conductor thickness is set to 10 μm. Ferroelectric bars' width and thickness are optimized to give a high Q.

Figure 7 shows the response of a multilayer filter depicted in Figure 6. Here, a hairpin with 2 μm thick $BaSrTiO_3$ is used.

This picture also shows the new response when a 3-micron $KTaO_3$ is inserted in the middle of the $BaSrTiO_3$ layer. The figure indicates an improvement in Q of up to 20%. The resonant frequency shifted downward as expected.

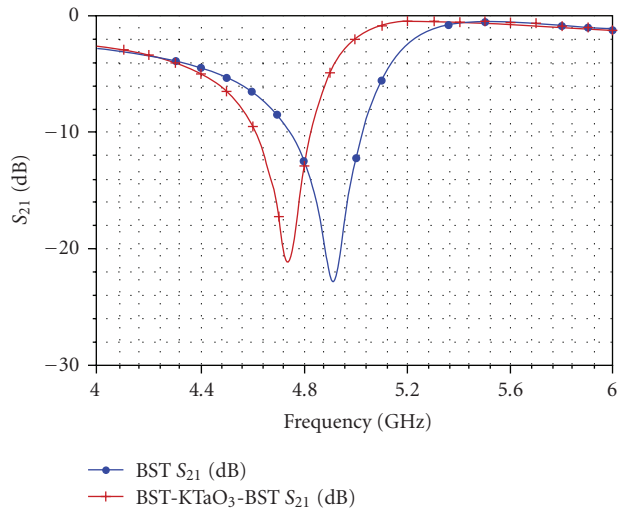

Figure 7: Frequency response of a multilayer structure.

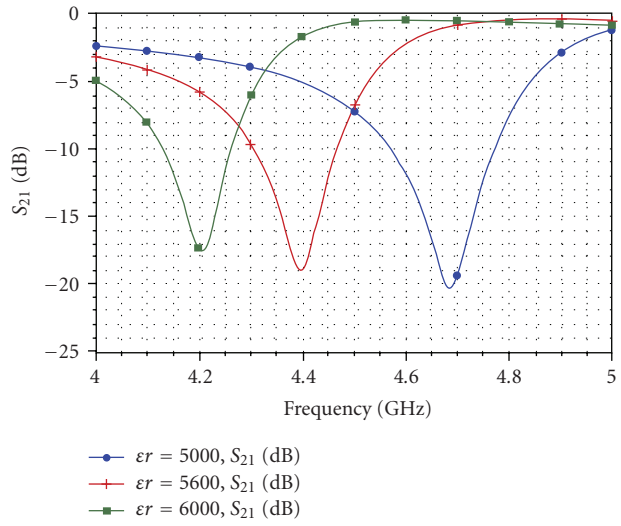

Figure 8: Frequency response (S_{21} (dB))—of tunable multilayer structure.

Subsequently, the tunableness of the multilayer structure is tested by applying a DC voltage between the hairpin and the ground plane of the microstrip line.

A decent tunableness in the order of 5% is predicted for a 20 volt variation in the DC voltage as shown in Figure 8.

4. LTCC SUBSTRATE CONFIGURATION

LTCC is a multilayer ceramic substrate technology. The multilayer architecture can be produced using stacked ceramic tapes that are used to apply conductive, dielectric, and/or resistive parts. These single sheets have to be laminated together and fired in one step at a relatively low temperature. This saves time, money, and reduces circuit dimensions. LTCC technology offers a high level of integration, buried

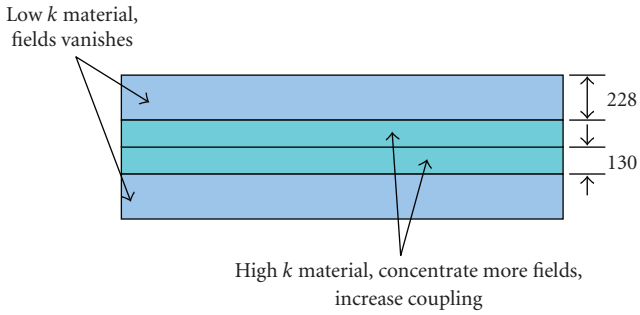

Figure 9: Cross-section of substrate layers using LTCC technology.

Table 1: LTCC material properties.

Kind of tape	k @ 2.5 GHz	Loss Factor @ 2.5 GHz
Hertape CT 707	6.37	$4.56*10E-3$
Hertape 765	68.7	$1.73*10E-3$

components, low loss, and system robustness. LTCC technology has been established in mobile communication techniques in the frequency range of a few GHz. LTCC has been investigated and has developed a good reputation for the high-frequency applications. Examples include: WLAN at 5 GHZ [18], radar sensors at 24 GHz and 77 GHz [19], and digital radio networks operating from 20 to 60 GHz [20] have also been reported.

Advances in new materials and fabrication technologies opened a new window in improving filter performance. One of these technologies is LTCC. Due to its thick conductor, losses of the LTCC filter can be reduced. The filter size can be also reduced by using embedded high dielectric-constant substrates. Also, one of the major advantages of using LTCC is its low cost and short fabrication cycle. Filters presented in this paper are formed between a high k material ($k = 65$) followed by a low k material ($k = 6$). Figure 9 shows the cross-sectional area of the mixed k substrate.

Table 1 shows the material properties of the mixed k substrate measured at 2.5 GHz.

5. PROPERTIES OF HAIR-PIN RESONATOR FILTER

Figure 10 shows the concept of using a hair-pin line as a resonator to design a simple bandpass filter (BPF).

A single capacitively coupled hair-pin resonator is used. The folded resonator length is 8800 microns on the LTCC multilayer substrates that are described above. Dimensions of the filter were set to comply with the LTCC design rules. The spacing between the resonator and the capacitive feeds, S, is set to 125 microns, which is the minimum spacing between conductors. The thickness of the conductor is 10 microns. The filter was simulated using the HFSS package. The effective dielectric constant is $\varepsilon_{\text{eff}} = 40$ and gives a resonance around 2.66 GHz.

Since the opposite sides of the hairpin resonator have opposite potentials, there is a virtual ground created at the center of the resonator. This makes the filter similar to the comb line filter [9] and makes this filter appropriate for

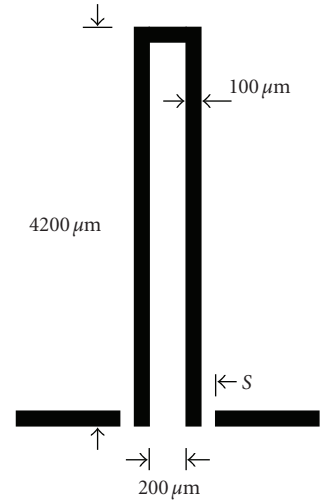

Figure 10: A single-resonator hair-pin filter with capacitance coupling at the input and output.

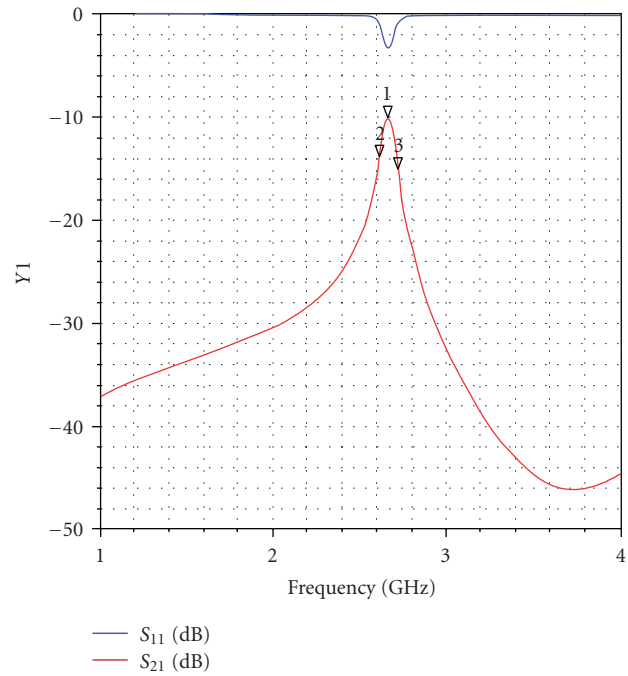

Figure 11: Simulated response of single hair-pin resonator filter with capacitive coupling.

planar applications that do not require vias connected to the ground plane.

Simulation results of the filter are shown in Figure 11.

It can be seen from the response of the filter that the insertion loss is very high ($\cong$ 10 dB). This is due to the weak coupling between the feeds and the resonator. Weak coupling is desirable for narrow-bandwidth filter, but it comes at the expense of increasing filter loss.

To further illustrate the effect of changing the spacing S, Table 2 shows performance of the filter for different values of S.

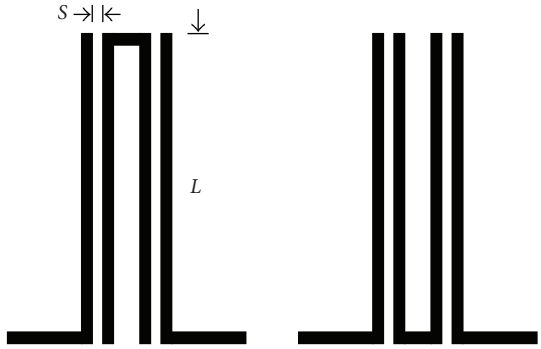

Figure 12: Single hair-pin resonator filter having two orientations with parallel coupled-feed lines.

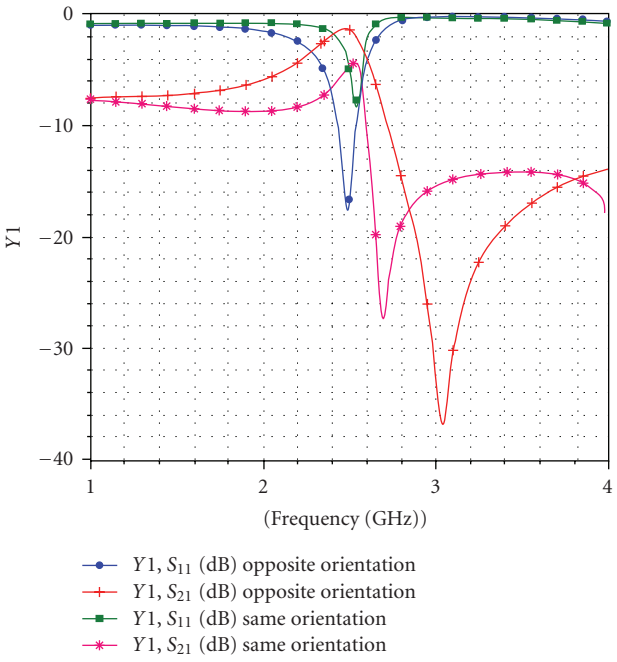

Figure 13: Simulated magnitude response of hair-pin resonator filter having two orientations with parallel coupled-feed lines.

Table 2: Effect of changing S on the filter response.

$S(\mu m)$	fr (GHz)	$I.L$ (dB)	$R.L.$ (dB)	3 dB-$B.W.$ (MHz)
100	2.66	10	3.31	73
50	2.65	6.9	5.17	80
25	2.61	6.25	5.91	91

It can be recognized from the table that there is a tradeoff between insertion loss and bandwidth.

The above discussion explains the basic operation of the hair-pin resonators. It is shown that narrow bandwidth can be obtained by using weak coupling at the expense of the insertion loss. This may render the filter useless in some applications. To increase coupling, parallel feed lines can be used to increase the coupling area. Figure 12 shows a single hair-pin filter with parallel feed lines.

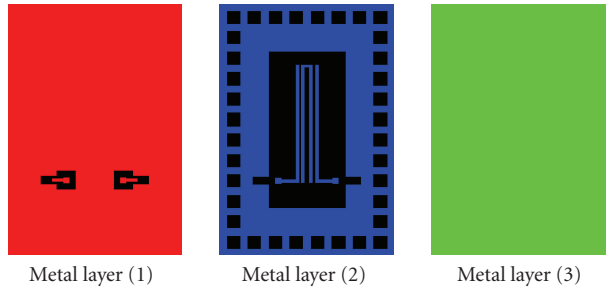

Figure 14: Configuration (1): metal layers.

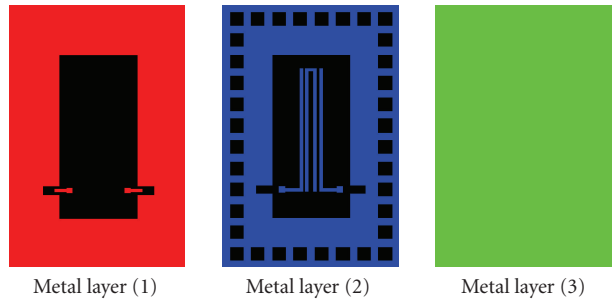

Figure 15: Configuration (2): metal layers.

While Figure 12 shows two different orientations of the resonator, with respect to the feed lines, in Figure 13 the responses of the filter are given.

It can be seen from the figure that if a resonator is in the same orientation as the feed line, then it has higher losses. This is because the crowding currents at coupling edges can increase loss [17]. A comparison between the two cases is shown in Table 3 in which the unloaded Q is higher for the opposite orientation.

6. FABRICATION AND MEASUREMENTS OF COUPLED-LINE FILTERS USING LTCC

The proposed coupled-line filter substrates will use embedded high dielectric material to reduce the size, and improve Q. Two filter configurations were considered in this layout. The first configuration is the strip-line configuration. A ground ring was formed around the filter to shield it and to connect the top and bottom metallization as shown in Figure 14.

In this layout, a minimum conductor width of 100 microns and a minimum metal spacing of 125 microns are considered. The second configuration is the microstrip configuration which was the same as configuration (1) without the top ground plane. The metallization of all layers for the second configuration is shown in Figure 15.

With a patch area of 76 mm by 76 mm, several filter structures using strip-line and microstrip, along with a calibration structure, were included in the layout. The latter is done for on-chip calibration and to exclude any parasitic effects in the measurement.

Table 3: Properties of the hair-pin resonator filter having two orientations with parallel coupled-feed lines.

	fr (GHz)	*I.L* (dB)	*R.L.* (dB)	3 dB-*B.W.* (MHz)	*Ql*	*Qul*
Opposite orientation	2.47	1.31	17.6	400	6.2	44.2
Same orientation	2.53	4.18	8.39	220	11.5	30.1

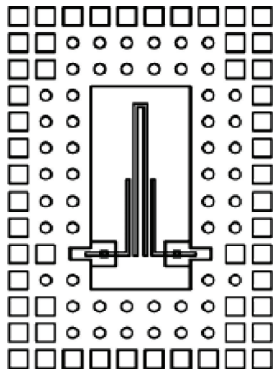

Figure 16: Layout of single hair-pin filter with parallel coupled-feed lines.

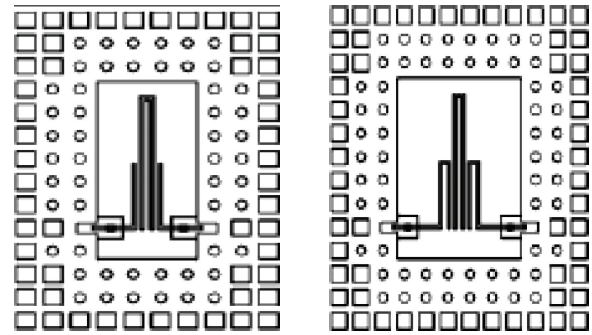

Figure 18: Single hair-pin resonator filter with (a) coupled-line feed and (b) loop.

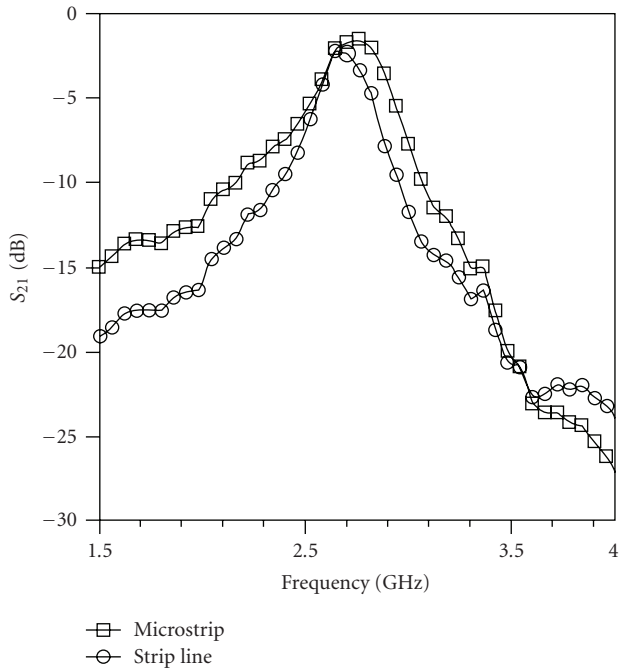

Figure 17: S_{21} for single hair-pin filter with (a) strip line, and with (b) microstrip line configuration.

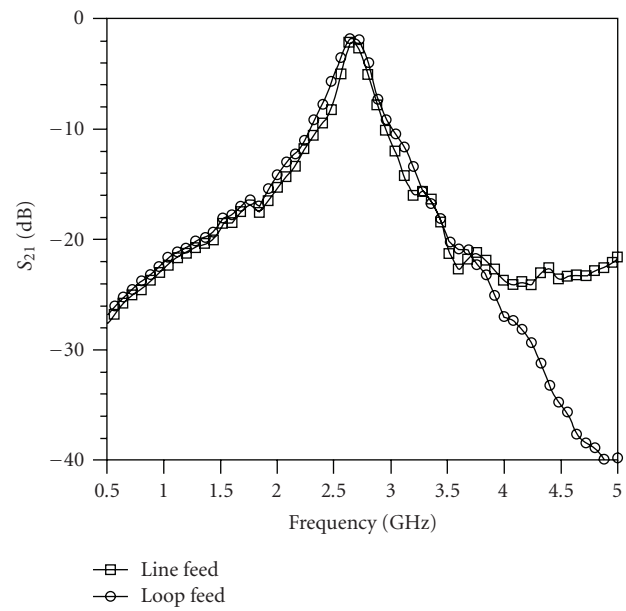

Figure 19: S_{21} for hair-pin resonator filter with (a) coupled-line feed and (b) loop feeds.

In the following, the measurement results of several coupled-line filters implemented using the mixed-*k* topology are reported.

6.1. Strip-line versus microstrip

Following the discussion in Section 4 about the parasitic effects on the filter performance, a single hair-pin resonator filter with line feed was implemented in both the strip-line and the microstrip configurations. Figure 16 shows the filter layout.

The line feed was about a quarter the length of the hair pin ($\approx \lambda/8$). As predicted previously, the microstrip configuration gave lower losses and a better quality factor than the strip-line configuration due to lower loss in the ground plane. Figure 17 shows the S_{21} for both configurations.

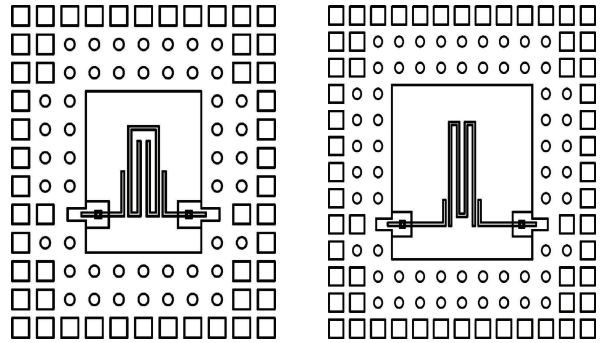

Figure 20: (a) Folded resonator, (b) W-shape resonator.

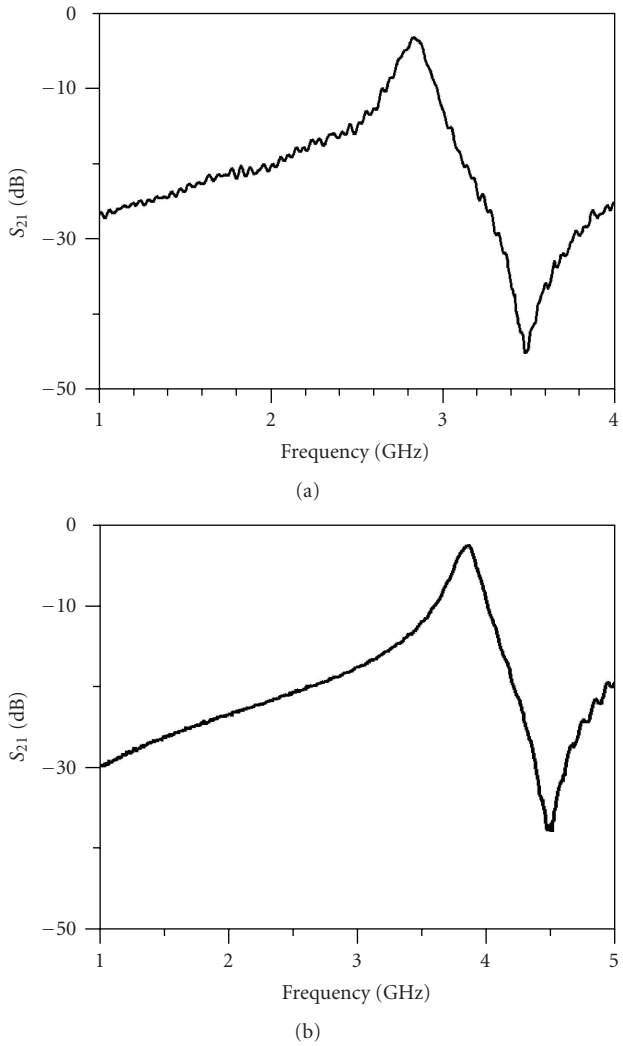

Figure 21: S_{21} (dB) for (a) capacitive (folded resonator) and (b) W-shape resonator.

6.2. Loop feeds versus coupled-line feeds

To investigate the feasibility of using a loop feed instead of a coupled-line feed, a hair-pin resonator filter was fabricated using coupled line and loop feeds. Figure 18 shows the filter layout.

The filter responses are shown in Figure 19.

6.3. W-shape resonator

To reduce the size and increase Q, a new resonator configuration using the W-shape is presented and compared to the existing folded resonator shape as shown in Figure 20.

Results show (see Figure 21) that the W-shape resonator filter gives a quality factor of 79 compared to the folded resonator that gave a quality factor of about 58. The higher resonance frequency of the W-shape as compared to the folded resonator was an indication of less capacitance.

7. CONCLUSION

In this paper, integration of passive filters on silicon substrates is investigated. Simple hair-pin band reject filters (BRFs), that support dielectric mode, are presented. Ferroelectric bars were used as resonant elements, compared to transmission line hair-pin resonators; an improvement of about 10 in Q is achieved. Multilayer dielectric ferroelectric material is discussed and gives about 5% tunableness. Furthermore, the miniaturization of filters introduced was achieved by using an embedded high-k substrate configuration that is feasible using an LTCC process. An improved W-shape bandpass filter was proposed with a wide stopband and approximately 5% bandwidth.

ACKNOWLEDGMENTS

The authors are thankful to the German Government (DFG) for supporting this project. It was performed in frame of a visiting professorship with Duisburg-Essen University, Campus Duisburg, under Subject no. Du 128/15-1.

REFERENCES

[1] S. B. Cohn, "Parallel-coupled transmission-line-resonator filters," *IRE Transactions on Microwave Theory and Techniques*, vol. 6, no. 2, pp. 223–231, 1998.

[2] E. G. Cristal and S. Frankel, "Hairpin-line and hybrid hairpin-line/half-wave parallel-coupled-line filters," *IEEE Transactions on Microwave Theory and Techniques*, vol. 20, no. 11, pp. 719–728, 1972.

[3] A. E. Williams, "A four-cavity elliptic waveguide filter," *IEEE Transactions on Microwave Theory and Techniques*, vol. 18, no. 12, pp. 1109–1114, 1970.

[4] J. B. Thomas, "Cross-coupling in coaxial cavity filters—a tutorial overview," *IEEE Transactions on Microwave Theory and Techniques*, vol. 51, no. 4, part 2, pp. 1368–1376, 2003.

[5] R. Levy, "Filters with single transmission zeros at real or imaginary frequencies," *IEEE Transactions on Microwave Theory and Techniques*, vol. 24, no. 4, pp. 172–181, 1976.

[6] U. Rosenberg and S. Amari, "Novel coupling schemes for microwave resonator filters," in *IEEE MTT-S International Microwave Symposium Digest*, vol. 3, pp. 1605–1608, Seattle, Wash, USA, June 2002.

[7] M. Makimoto and S. Yamashita, "Bandpass filters using parallel coupled stripline stepped impedance resonators," *IEEE Transactions on Microwave Theory and Techniques*, vol. 28, no. 12, pp. 1413–1417, 1980.

[8] M. Sagawa, K. Takahashi, and M. Makimoto, "Miniaturized hairpin resonator filters and their application to receiver front-end MICs," *IEEE Transactions on Microwave Theory and Techniques*, vol. 37, no. 12, pp. 1991–1997, 1989.

[9] G. L. Matthaei, N. O. Fenzi, R. J. Forse, and S. M. Rohfing, "Hairpin-comb filters for HTS and other narrow-band applications," *IEEE Transactions on Microwave Theory and Techniques*, vol. 45, no. 8, part 1, pp. 1226–1231, 1997.

[10] J.-S. Hong and M. J. Lancaster, "Theory and experiment of novel microstrip slow-wave open-loop resonator filters," *IEEE Transactions on Microwave Theory and Techniques*, vol. 45, no. 12, part 2, pp. 2358–2365, 1997.

[11] J.-S. Park, J.-S. Yun, and D. Ahn, "A design of the novel coupled-line bandpass filter using defected ground structure with wide stopband performance," *IEEE Transactions on Microwave Theory and Techniques*, vol. 50, no. 9, pp. 2037–2043, 2002.

[12] G. L. Matthaei, "Narrow-band, fixed-tuned, and tunable bandpass filters with zig-zag hairpin-comb resonators," *IEEE Transactions on Microwave Theory and Techniques*, vol. 51, no. 4, part 1, pp. 1214–1219, 2003.

[13] E. G. Cristal, "Tapped-line coupled transmission lines with applications to interdigital and combline filters," *IEEE Transactions on Microwave Theory and Techniques*, vol. 23, no. 12, pp. 1007–1012, 1975.

[14] J. S. Wong, "Microstrip tapped-line filter design," *IEEE Transactions on Microwave Theory and Techniques*, vol. 27, no. 1, pp. 44–50, 1979.

[15] G. Torregrosa-Penalva, G. López-Risueño, and J. I. Alonso, "A simple method to design wide-band electronically tunable combline filters," *IEEE Transactions on Microwave Theory and Techniques*, vol. 50, no. 1, pp. 172–177, 2002.

[16] I. Vendik, O. Vendik, V. Pleskachev, A. Svishchev, and R. Wördenweber, "Design of tunable ferroelectric filters with a constant fractional band width," in *IEEE MTT-S International Microwave Symposium Digest*, vol. 3, pp. 1461–1464, Phoenix, Ariz, USA, May 2001.

[17] A. Tombak, F. T. Ayguavives, J.-P. Maria, G. T. Stauf, A. I. Kingon, and A. Mortazawi, "Tunable RF filters using thin film barium strontium titanate based capacitors," in *IEEE MTT-S International Microwave Symposium Digest*, vol. 3, pp. 1453–1456, Phoenix, Ariz, USA, May 2001.

[18] L. Lecheminoux and N. Gosselin, "Advanced design, technology & manufacturing for high volume and low cost production," in *Proceedings of the IEEE/CPMT 28th International Electronics Manufacturing Technology Symposium (IEMT '03)*, pp. 255–260, San Jose, Calif, USA, July 2003.

[19] S. Holzwarth, R. Kulke, J. Kassner, and P. Uhlig, "Antenna integration on LTCC radar module for automotive applications at 24 GHz," in *The IMAPS Nordic Conference*, Helsingør, Denmark, September 2004.

[20] R. Kulke, G. Möllenbeck, W. Simon, A. Lauer, and M. Rittweger, "Point-to-multipoint transceiver in LTCC for 26 GHz," in *The IMAPS Nordic Conference*, pp. 50–53, Stockholm, Sweden, September-October 2002.